nature immunology

# Dipeptidylpeptidase 4 inhibition enhances lymphocyte trafficking, improving both naturally occurring tumor immunity and immunotherapy

Rosa Barreira da Silva[1,2], Melissa E Laird[1,2], Nader Yatim[1,2], Laurence Fiette[3,4], Molly A Ingersoll[1,2] & Matthew L Albert[1,2]



**The success of antitumor immune responses depends on the infiltration of solid tumors by effector T cells, a process guided by chemokines. Here we show that *in vivo* post-translational processing of chemokines by dipeptidylpeptidase 4 (DPP4, also known as CD26) limits lymphocyte migration to sites of inflammation and tumors. Inhibition of DPP4 enzymatic activity enhanced tumor rejection by preserving biologically active CXCL10 and increasing trafficking into the tumor by lymphocytes expressing the counter-receptor CXCR3. Furthermore, DPP4 inhibition improved adjuvant-based immunotherapy, adoptive T cell transfer and checkpoint blockade. These findings provide direct *in vivo* evidence for control of lymphocyte trafficking via CXCL10 cleavage and support the use of DPP4 inhibitors for stabilizing biologically active forms of chemokines as a strategy to enhance tumor immunotherapy.**

Chemokines regulate leukocyte trafficking in healthy tissues (homeostatic chemokines) and in response to stress, infection or tissue damage (inflammatory chemokines)[1]. Although the mechanisms supporting chemokine-induced leukocyte motility (chemokinesis) and directed migration (chemotaxis) have been described[2], less is known about how naturally occurring post-translational modifications regulate these mechanisms. It is known that chemokine activity can be influenced by post-translational modifications[3,4], but the lack of direct *in vivo* evidence has limited the impact of these *in vitro* biochemical observations on both the field of chemotaxis and the development of novel immunotherapies.

DPP4 (also known as CD26) is an X-prolyl dipeptidylpeptidase capable of enzymatically removing the first two amino acids from a protein that possesses a proline or alanine in the penultimate N-terminal position[5]. Under steady-state conditions, DPP4 is enzymatically active as both a membrane-bound protein and a soluble protein, and it is expressed in several tissues and biological fluids in the body[6]. DPP4 expression and/or activity can be affected by inflammation and malignant transformation[7,8]. Although DPP4 has been documented as an important diagnostic or prognostic biomarker in several clinical settings, its role in regulating protein function in the context of disease pathogenesis is largely unknown. The one disease setting in which DPP4 has been extensively studied is type II diabetes. N-terminal truncation of the incretin hormones glucose-dependent insulinotropic polypeptide and glucagon-like peptide 1 leads to the formation of antagonist forms and constitutes a mechanism of insulin resistance. Accordingly, DPP4 inhibitors have been developed and approved as treatments for type II diabetes[9].

In addition to the incretin hormones, other secreted molecules possess the N-terminal consensus motif for DPP4 recognition. Notably, several chemokines have been shown to be processed *in vitro* by DPP4 (refs. 3,10). Among these, the proinflammatory chemokine CXCL10 was shown to be readily truncated *in vitro*. This generated an antagonist form that is capable of engaging its receptor, CXCR3, but does not induce chemotaxis[4]. Published studies of chronic hepatitis C suggest that this phenomenon might have relevance in disease pathogenesis. Specifically, high concentrations of N-terminally truncated CXCL10 were correlated with treatment failure[11,12]. Moreover, subjects that did not respond to treatment showed higher concentrations of soluble DPP4 than did those subjects that achieved viral clearance[12,13]. Other characterized chemokine substrates include CXCL12, whose truncation by DPP4 is believed to regulate mobilization of CXCR4-expressing hematopoietic stem cells by the cell-signaling molecules G-CSF and GM-CSF[14]. CCL22 and CCL5 are two additional examples that have been evaluated *in vitro*[10,15]; however, *in vivo* evidence of altered leukocyte trafficking is thus far lacking.

Here we tested the hypothesis that DPP4 regulates chemokine-mediated lymphocyte trafficking into inflammatory sites, such as the tumor parenchyma. Our findings provide direct evidence that DPP4 inhibition protects the biologically active form of CXCL10, which in turn enhances the recruitment of lymphocytes into the tumor parenchyma. DPP4 inhibitors, including sitagliptin (currently approved for use in type II diabetes), also enhanced the effect of three distinct immunotherapy strategies. These results support the idea of a functional role for DPP4-mediated post-translational modification of chemokines in

[1]Laboratory of Dendritic Cell Immunobiology, Institut Pasteur, Paris, France. [2]Inserm U818, Paris, France. [3]Human Histopathology and Animal Models, Institut Pasteur, Paris, France. [4]Université Paris Descartes–Sorbonne Paris Cité, Paris, France. Correspondence should be addressed to M.L.A. (albertm@pasteur.fr).

Received 30 March; accepted 17 May; published online 15 June 2015; doi:10.1038/ni.3201

the regulation of tumor immunity. Our findings establish preclinical support for the repurposing of DPP4 inhibitors, which can be used to direct effector-cell migration in the context of tumor immunotherapy.

## RESULTS

### DPP4 inhibition enhances antitumor responses to melanoma

Despite data suggesting that T cell infiltration into solid tumors is a correlate of better prognosis[16,17], there is no known therapeutic approach for directing lymphocytes into the tumor parenchyma. As the enzyme DPP4 was shown to modulate the activity of several immune molecules (including proinflammatory chemokines), we evaluated its role in tumorigenesis. First, we studied DPP4 expression in B16F10 tumor cells by flow cytometry. Although DPP4 was not expressed by *in vitro*–cultured B16F10 cells (**Supplementary Fig. 1a**), we detected high DPP4 activity and expression in excised B16F10 subcutaneous tumors by enzymatic assay and enzyme-linked immunosorbent assay (ELISA), respectively (**Fig. 1a** and **Supplementary Fig. 1b**). Notably, tumor-associated DPP4 activity was detectable but considerably lower when tumors were implanted into *Dpp4*$^{-/-}$ mice, which suggested a contribution from both tumor cells and tumor-induced stroma. Next, we evaluated whether DPP4 expression has a role in tumorigenesis by comparing tumor growth in *Dpp4*$^{-/-}$ mice to that in heterozygote littermates. We observed a significant delay in tumor growth when DPP4 was absent (**Fig. 1b**). To specifically evaluate the role of DPP4 enzymatic activity, we fed wild-type mice with chow formulated to contain a DPP4-specific inhibitor called sitagliptin (also known by its trade name, Januvia). Using sitagliptin chow also allowed us to circumvent possible caveats related to developmental differences between wild-type and *Dpp4*$^{-/-}$ mice. More than 80% of *in vivo* enzymatic activity was inhibited in mice fed sitagliptin chow (**Fig. 1c**), with no evidence of long-term drug intolerance or toxicity. Furthermore, we observed reduced DPP4 enzymatic activity in melanoma tumors extracted from the mice (**Fig. 1d**). Notably, *in vivo* DPP4 inhibition resulted in reduced tumor growth (**Fig. 1e**). By contrast, sitagliptin treatment of *Dpp4*$^{-/-}$ mice did not influence the kinetics of melanoma growth (**Supplementary Fig. 1c**), which allowed us to rule out off-target effects or direct cytotoxicity of the drug on the tumor.

To evaluate DPP4 inhibition as a treatment for established tumors, we fed sitagliptin chow to mice 3, 5 or 7 d after orthotopic tumor implantation. We observed a delay in tumor growth when sitagliptin was administered within 5 d after tumor-cell implantation

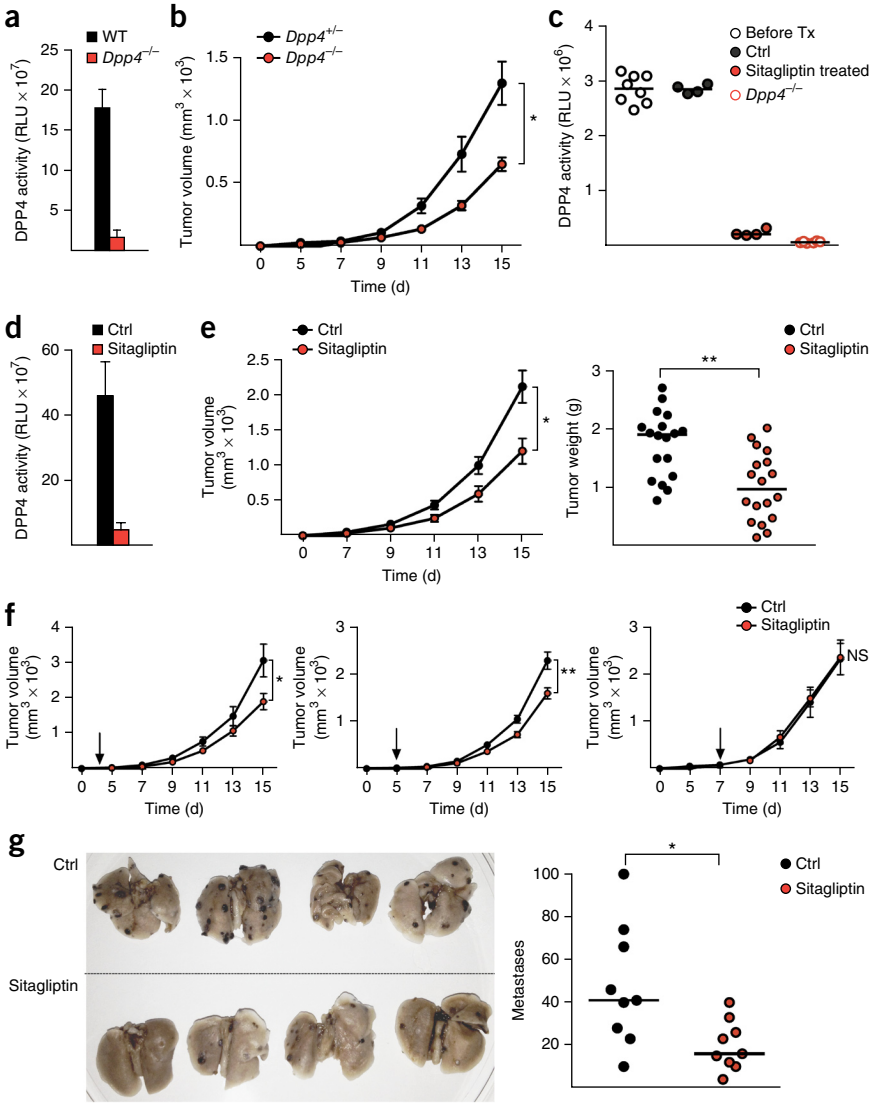


**Figure 1** Inhibition of DPP4 enhances naturally occurring antitumor responses to B16F10 melanoma. (**a**) C57BL/6 wild-type (WT) and *Dpp4*$^{-/-}$ mice were subcutaneously injected with B16F10 cells. Eight days after injection, tumor homogenates were prepared and DPP4 activity was determined. RLU, relative luminescence units. Data represent mean ± s.e.m. $n = 3$ (WT) and 4 (*Dpp4*$^{-/-}$) mice. (**b**) Tumor cells were transferred into *Dpp4*$^{+/-}$ and *Dpp4*$^{-/-}$ mice as described for **a**. Tumor volumes are shown (mean ± s.e.m.; $n = 6$ mice per group). $^{*}P < 0.01$. (**c**) WT mice were fed with chow containing 1.1% sitagliptin or with control chow (Ctrl). DPP4 activity was measured in plasma samples collected before and 24 h after the initiation of treatment (Tx). DPP4 plasma activity is shown for *Dpp4*$^{-/-}$ mice and used as a reference for the absence of activity. Each circle represents an individual mouse. (**d**,**e**) DPP4 activity in tumor homogenates (**d**) and day 15 tumor volumes and weights (**e**) in WT mice receiving control or sitagliptin diet that were subcutaneously injected as described in **a**. Data represent mean ± s.e.m. $n = 4$ mice per group in **d** and 18 mice per group in **e**. $^{*}P < 0.01$, $^{**}P < 0.005$. (**f**) Tumor volumes in WT mice with growing B16F10 tumors fed sitagliptin chow at days 3, 5 and 7 (arrows). Data represent mean ± s.e.m.; $n = 12$, 13 and 7 mice per group from left to right. $^{*}P < 0.05$, $^{**}P < 0.01$. NS, not significant ($P > 0.05$). (**g**) Lungs of control and sitagliptin-fed WT mice intravenously injected with $2 \times 10^5$ B16F10 cells. Shown are representative images of lungs from four mice per group dissected 15 d after injection. Data for all mice are plotted (right), with each circle indicating the number of metastases in a single mouse ($n = 9$ mice per group; $^{*}P < 0.05$). Significance was determined by two-way analysis of variance (ANOVA) (**b**, **e** (left) and **f**) or Mann-Whitney test (**e** (right) and **g**). Data shown are representative of two (**a**, **b** and **d**) or eight experiments (**c**) or are pooled from three (**e**) or two (**f**,**g**) independent experiments.

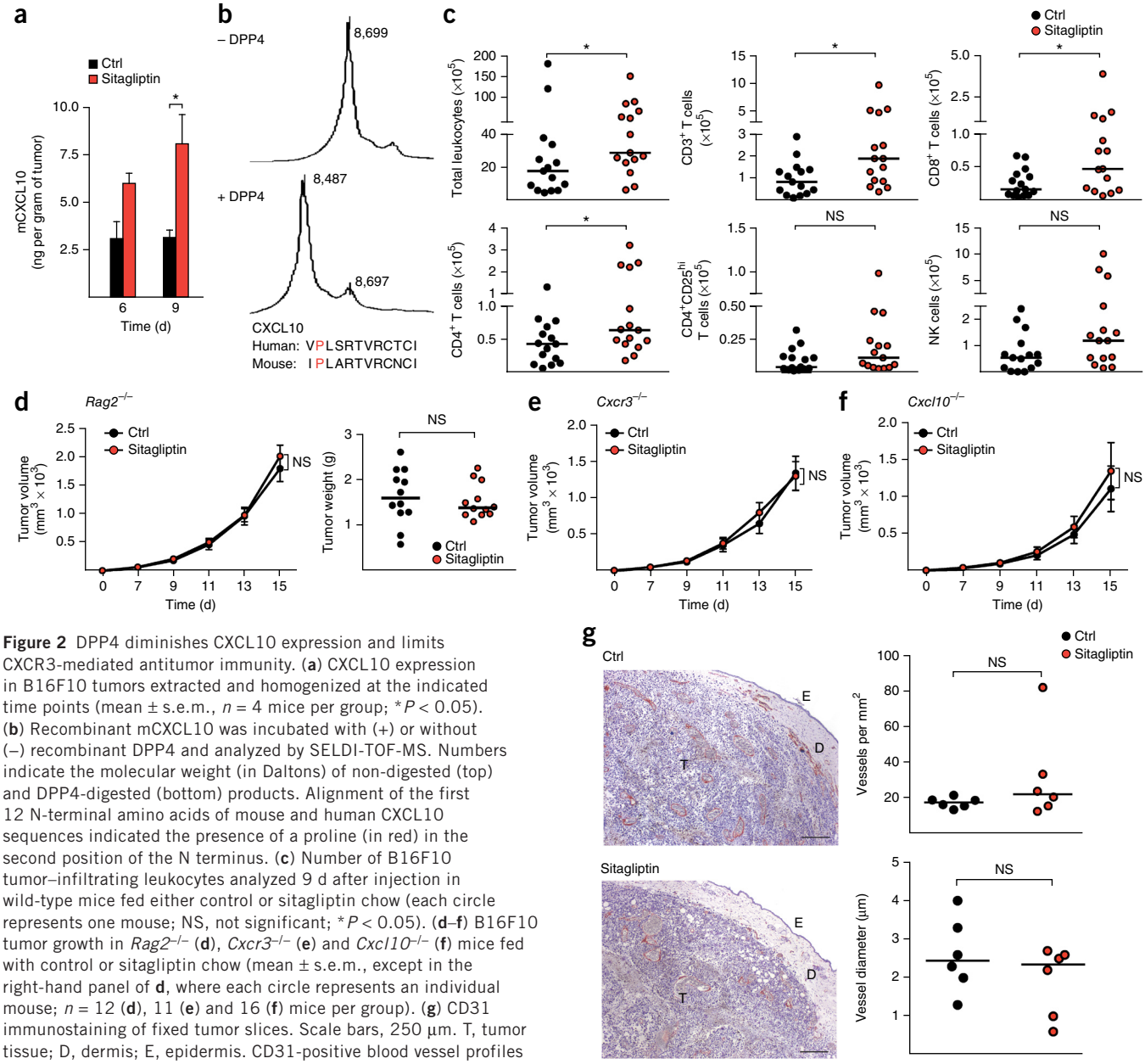


**Figure 2** DPP4 diminishes CXCL10 expression and limits CXCR3-mediated antitumor immunity. (**a**) CXCL10 expression in B16F10 tumors extracted and homogenized at the indicated time points (mean ± s.e.m., $n = 4$ mice per group; $^*P < 0.05$). (**b**) Recombinant mCXCL10 was incubated with (+) or without (–) recombinant DPP4 and analyzed by SELDI-TOF-MS. Numbers indicate the molecular weight (in Daltons) of non-digested (top) and DPP4-digested (bottom) products. Alignment of the first 12 N-terminal amino acids of mouse and human CXCL10 sequences indicated the presence of a proline (in red) in the second position of the N terminus. (**c**) Number of B16F10 tumor–infiltrating leukocytes analyzed 9 d after injection in wild-type mice fed either control or sitagliptin chow (each circle represents one mouse; NS, not significant; $^*P < 0.05$). (**d**–**f**) B16F10 tumor growth in *Rag2*$^{-/-}$ (**d**), *Cxcr3*$^{-/-}$ (**e**) and *Cxcl10*$^{-/-}$ (**f**) mice fed with control or sitagliptin chow (mean ± s.e.m., except in the right-hand panel of **d**, where each circle represents an individual mouse; $n = 12$ (**d**), 11 (**e**) and 16 (**f**) mice per group). (**g**) CD31 immunostaining of fixed tumor slices. Scale bars, 250 μm. T, tumor tissue; D, dermis; E, epidermis. CD31-positive blood vessel profiles were counted and measured as described in the Online Methods. Each circle represents a single mouse. Significance was determined via Mann-Whitney test (**a**, **c**, **d** (right) and **g**) or two-way ANOVA (**d** (left), **e** and **f**). Data are representative of three (**b**) or two (**a**,**g**) experiments or are pooled from three (**c**,**f**) or two (**d**,**e**) independent experiments.

(**Fig. 1f**). Finally, we assessed DPP4 inhibition in a model of metastatic melanoma achieved by intravenous injection of B16F10 cells. DPP4 inhibition significantly reduced the number of lung metastases in treated mice compared with control mice (**Fig. 1g**). These results suggest a role for DPP4 as a regulator of tumor growth in both orthotopic and metastatic models.

### Enhanced CXCL10- and CXCR3-dependent tumor immunity

*In vitro* biochemical studies have established that DPP4 truncates chemokines and other immune molecules, initiating their catabolism and clearance by other N-terminal aminopeptidases[18]. To gain insight into the mechanism(s) responsible for delayed melanoma growth, we excised tumors growing in control and sitagliptin-treated mice and quantified the expression of known DPP4 substrates. We observed elevated concentrations of tumor-associated mouse CXCL10 (mCXCL10) in B16F10 tumors growing in sitagliptin-treated mice, whereas the concentrations of mCCL2, mCCL22 and vascular endothelial growth factor (VEGF) were similar in treated and control animals (**Fig. 2a** and **Supplementary Fig. 2a**). Of note, the potential DPP4 substrates mCXCL12 and mCCL3 were undetectable in the extracted tumors (data not shown). The *in vivo* protection of CXCL10 by sitagliptin was consistent with mCXCL10 being a substrate for DPP4 (**Fig. 2b**). Notably, mCXCL10 is the only CXCR3 ligand sensitive to DPP4 N-terminal truncation (**Supplementary Fig. 2b**). Despite the lack of a higher chemokine concentration *in vivo*, we confirmed the *in vitro* cleavage of putative DPP4 substrates that contain the X-proline

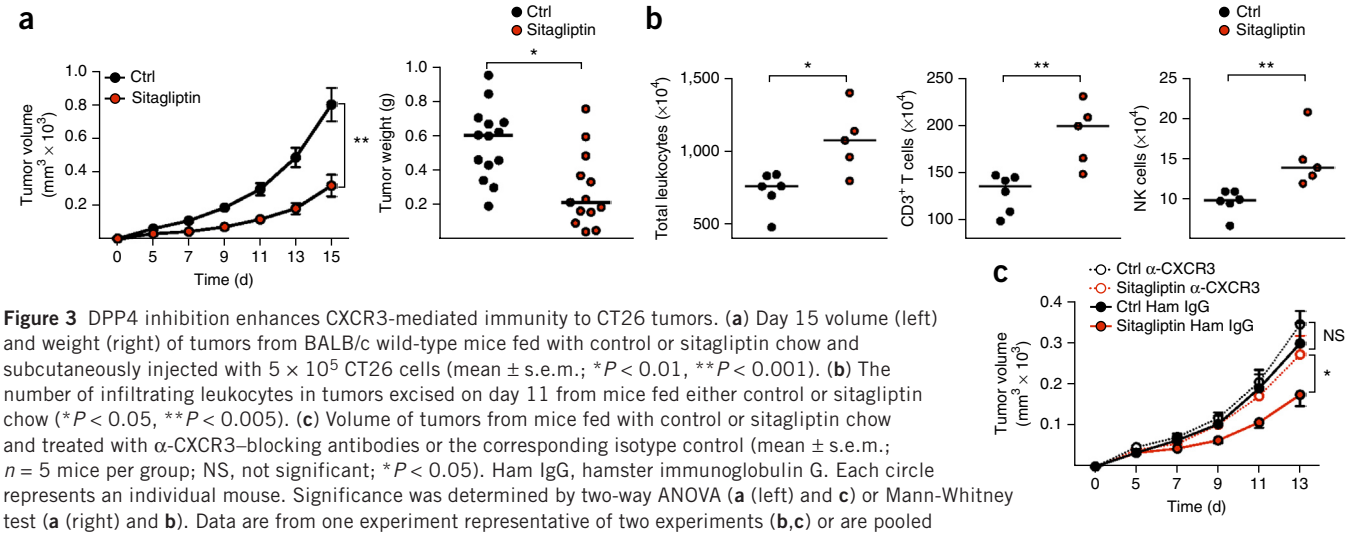


**Figure 3** DPP4 inhibition enhances CXCR3-mediated immunity to CT26 tumors. (**a**) Day 15 volume (left) and weight (right) of tumors from BALB/c wild-type mice fed with control or sitagliptin chow and subcutaneously injected with $5 \times 10^5$ CT26 cells (mean ± s.e.m.; $^*P < 0.01$, $^{**}P < 0.001$). (**b**) The number of infiltrating leukocytes in tumors excised on day 11 from mice fed either control or sitagliptin chow ($^*P < 0.05$, $^{**}P < 0.005$). (**c**) Volume of tumors from mice fed with control or sitagliptin chow and treated with α-CXCR3–blocking antibodies or the corresponding isotype control (mean ± s.e.m.; $n = 5$ mice per group; NS, not significant; $^*P < 0.05$). Ham IgG, hamster immunoglobulin G. Each circle represents an individual mouse. Significance was determined by two-way ANOVA (**a** (left) and **c**) or Mann-Whitney test (**a** (right) and **b**). Data are from one experiment representative of two experiments (**b**,**c**) or are pooled from two independent experiments (**a**).

N-terminal motif—mCCL2, mCXCL12, mCCL22, and three other β-chemokines, mCCL3, mCCL4 and mCCL5 (**Supplementary Fig. 2c**).

Higher concentrations of CXCL10 correlated with a significant increase in the number of $CD4^+$ and $CD8^+$ T cells localized to the tumors of sitagliptin-treated animals (**Fig. 2c** and **Supplementary Fig. 2d**). By contrast, no major differences were seen in the numbers of tumor-infiltrating myeloid cells, NK cells, B lymphocytes and $CD25^{hi}$ regulatory T cells (**Fig. 2c** and data not shown). To directly assess increased lymphocyte trafficking as the mechanism of action by which DPP4 inhibition influences tumor growth, we injected B16F10 melanoma cells into *Rag2*$^{-/-}$ mice that had been fed either sitagliptin or control chow. In the absence of adaptive immunity, the beneficial effects of DPP4 inhibition were lost (**Fig. 2d**). These results supported a role for immune cells and prompted us to assess chemokine-mediated lymphocyte trafficking as the mechanism of action by which sitagliptin mediates tumor immunity.

The migration of activated or memory lymphocytes is typically mediated by α- and β-chemokines[1], some of which are DPP4 substrates (**Supplementary Fig. 2b**,**c**). We therefore tested whether CXCR3 or CCR5 mediated the observed tumor immunity in sitagliptin-treated mice. The absence of CXCR3 (tested with *Cxcr3*$^{-/-}$ mice) abrogated the delay in tumor growth achieved through DPP4 inhibition (**Fig. 2e**). By contrast, CCR5 blockade or the use of *Ccr5*$^{-/-}$ mice led to maintenance of a beneficial effect of sitagliptin similar to that seen in control or wild-type mice (**Supplementary Fig. 3a**,**b**). As mCXCL10 is the sole CXCR3 ligand that can be post-translationally modified by DPP4, we next tested *Cxcl10*$^{-/-}$ mice. Similar to findings in *Cxcr3*$^{-/-}$ mice, the delayed tumor growth achieved with DPP4 inhibition was absent in *Cxcl10*$^{-/-}$ mice (**Fig. 2f**). Notably, the tumor growth in *Cxcl10*$^{-/-}$ mice was delayed compared to that in wild-type mice, probably because the strain expresses a functional form of CXCL11 (ref. 19). Results were confirmed in wild-type animals treated with CXCL10-blocking antibodies (**Supplementary Fig. 3c**).

Although these data supported a direct role for DPP4 protection of CXCL10 in enhancing tumor immunity and infiltration by lymphocytes, we considered other possible mechanisms of action. First, we evaluated the reported angiostatic effects of CXCL10 (ref. 20). Histological analysis of tumors showed no difference between the

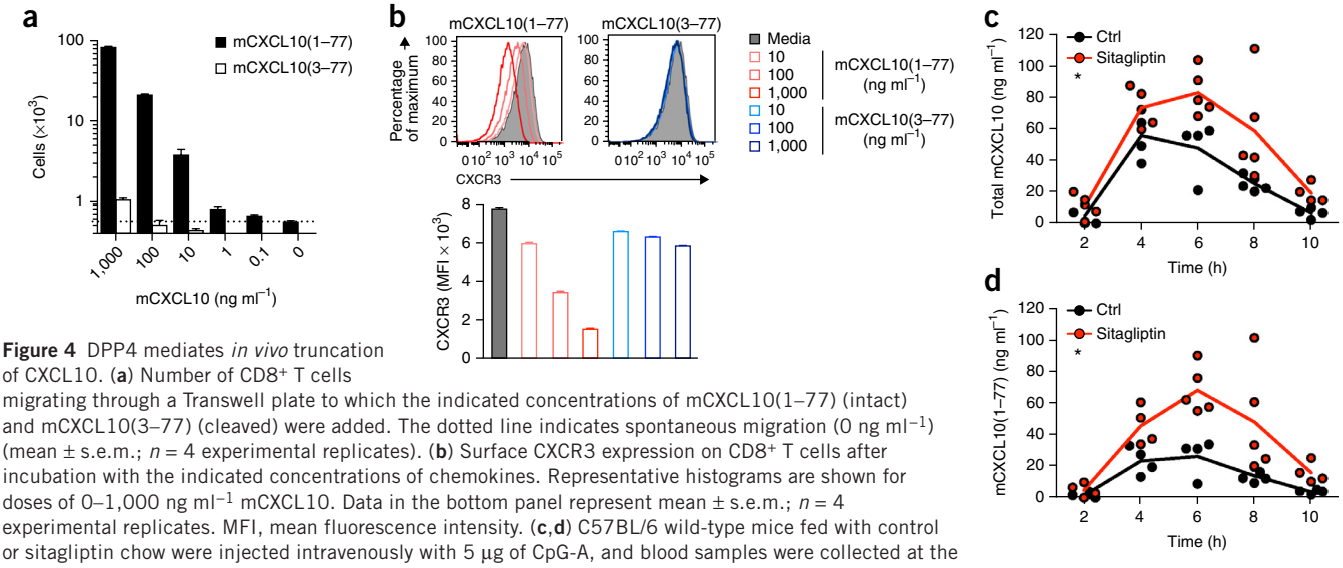


**Figure 4** DPP4 mediates *in vivo* truncation of CXCL10. (**a**) Number of $CD8^+$ T cells migrating through a Transwell plate to which the indicated concentrations of mCXCL10(1–77) (intact) and mCXCL10(3–77) (cleaved) were added. The dotted line indicates spontaneous migration (0 ng ml$^{-1}$) (mean ± s.e.m.; $n = 4$ experimental replicates). (**b**) Surface CXCR3 expression on $CD8^+$ T cells after incubation with the indicated concentrations of chemokines. Representative histograms are shown for doses of 0–1,000 ng ml$^{-1}$ mCXCL10. Data in the bottom panel represent mean ± s.e.m.; $n = 4$ experimental replicates. MFI, mean fluorescence intensity. (**c**,**d**) C57BL/6 wild-type mice fed with control or sitagliptin chow were injected intravenously with 5 μg of CpG-A, and blood samples were collected at the indicated time points. Plots show total mCXCL10 (**c**) and mCXCL10(1–77) (**d**) as determined by ELISA ($^*P < 0.01$). Each circle represents a single mouse. Significance was determined by two-way ANOVA. Data are representative of three (**a**,**b**) or two (**c**,**d**) independent experiments.

numbers and diameters of blood vessels (as measured by CD31 staining) present in the tumors of untreated and sitagliptin-treated mice (**Fig. 2g**). Furthermore, the concentration of tumor-associated VEGF was not altered by sitagliptin treatment (**Supplementary Fig. 2a**). Additionally, the fact that CXCL12 is a substrate of DPP4 (ref. 21) prompted us to consider the reported observation that CXCR4 antagonists modulate tumor growth. As indicated above, we did not detect CXCL12 expression within the growing tumors (data not shown). Moreover, blocking CXCR4 *in vivo* did not affect sitagliptin-mediated inhibition of tumor growth (**Supplementary Fig. 3d**). These results support our conclusion that the protection of CXCL10 within the tumor and CXCR3-directed migration of lymphocytes account for the enhanced tumor immunity noted when DPP4 activity is inhibited.

Our observations in the melanoma model prompted us to study whether DPP4-mediated antitumor immunity could be extended to other tumor models. We therefore employed the CT26 colon carcinoma cell line, which can be used to initiate subcutaneous tumors in BALB/c mice. DPP4 inhibition resulted in a marked delay of CT26 tumor growth (**Fig. 3a**), which correlated with enhanced infiltration of lymphocytes, including T cell subsets and NK cells (**Fig. 3b**). Of note, the absolute numbers of tumor-associated B cells, eosinophils and CD25$^{hi}$ regulatory T cells did not change after sitagliptin treatment (**Supplementary Fig. 4**). Blocking CXCR3-receptor signaling resulted in a loss of the protection achieved with DPP4 inhibition (**Fig. 3c**). Our results indicated that DPP4 acts to negatively regulate CXCR3-mediated antitumor immunity, effectively limiting lymphocyte infiltration into the tumor parenchyma.

## CXCL10 degradation limits the migration of CXCR3$^+$ lymphocytes

Most biochemical and functional studies of chemokine processing have used human proteins. Indeed, only a few mouse chemokines have been reported to be DPP4 substrates[21,22]. As indicated above, we directly tested the ability of DPP4 to truncate an extended panel of chemokines (**Fig. 2b** and **Supplementary Fig. 2b,c**). We further assessed the consequences of DPP4 post-translational modification on mCXCL10-induced lymphocyte trafficking. We examined the ability of full-length and DPP4-truncated mCXCL10 (referred to herein as mCXCL10(1–77) and mCXCL10(3–77), respectively) to promote lymphocyte migration in an *in vitro* Transwell system. Consistent with human studies[4], DPP4-truncated mCXCL10(3–77) did not induce T cell migration (**Fig. 4a**), nor did it trigger CXCR3 internalization (**Fig. 4b**).

To study whether DPP4 mediates the truncation of CXCL10 *in vivo*, we induced endogenous CXCL10 production by intravenous injection of the Toll-like receptor 9 agonist CpG-A. DPP4 inhibition resulted in the stabilization of CpG-A–induced plasma CXCL10 (referred to herein as total CXCL10 and detected by conventional assays that measured both intact and N-terminally truncated CXCL10) as compared with that in control wild-type mice (**Fig. 4c**). To quantify bioactive CXCL10, we established an immunoassay specific for

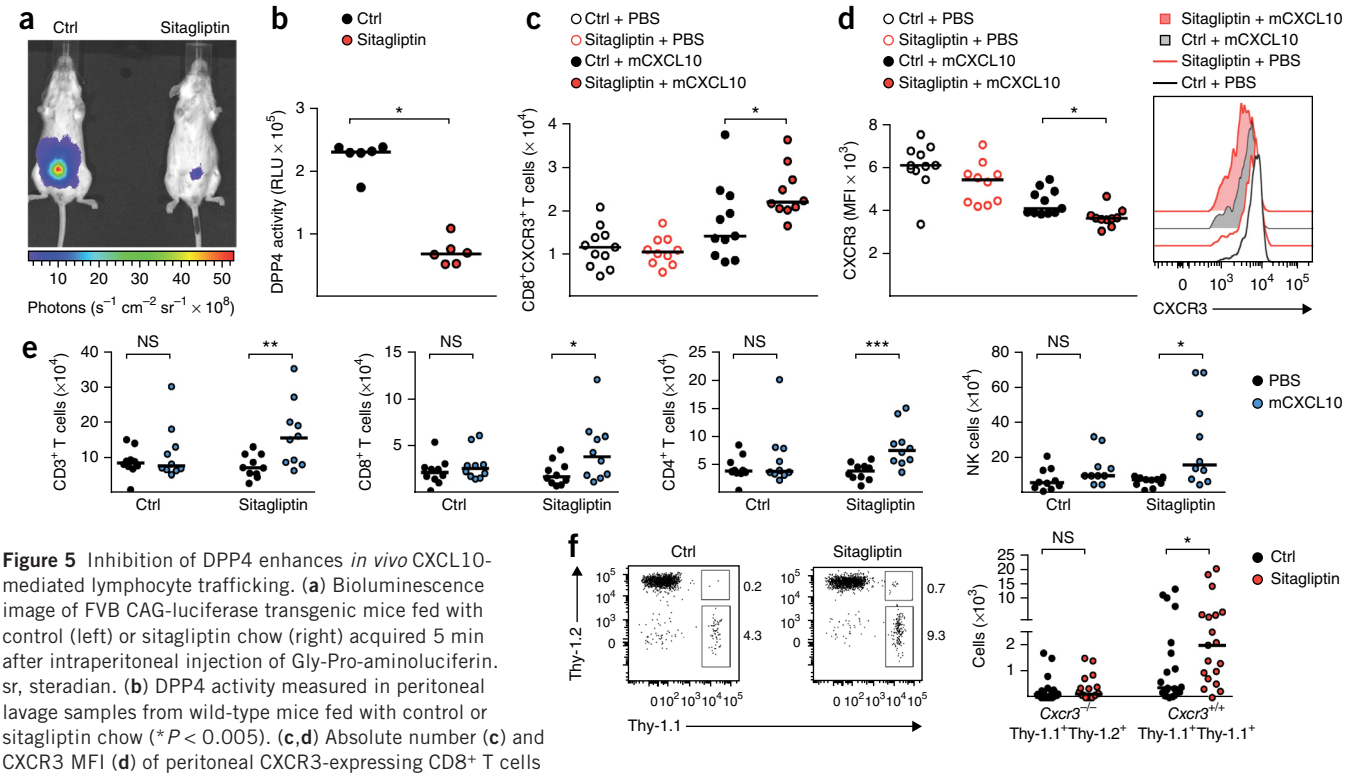


**Figure 5** Inhibition of DPP4 enhances *in vivo* CXCL10-mediated lymphocyte trafficking. (**a**) Bioluminescence image of FVB CAG-luciferase transgenic mice fed with control (left) or sitagliptin chow (right) acquired 5 min after intraperitoneal injection of Gly-Pro-aminoluciferin. sr, steradian. (**b**) DPP4 activity measured in peritoneal lavage samples from wild-type mice fed with control or sitagliptin chow (*$P < 0.005$). (**c**,**d**) Absolute number (**c**) and CXCR3 MFI (**d**) of peritoneal CXCR3-expressing CD8$^+$ T cells in wild-type mice fed with control or sitagliptin chow and injected intraperitoneally with PBS or recombinant mCXCL10. Representative histograms showing CXCR3 expression in CXCR3$^+$CD8$^+$ T cells are shown. **c**, *$P < 0.05$; **d**, *$P < 0.005$. (**e**) Endogenous lymphocytes in wild-type mice fed with control or sitagliptin food and growing B16F10 tumors that were given an intratumoral injection of PBS or mCXCL10 7 d after tumor-cell implant. NS, not significant; *$P < 0.05$, **$P < 0.01$, ***$P < 0.005$. (**f**) Three days after tumor-cell implantation, mice received an adoptive transfer of pmel-1 CD8$^+$ T cells from *Cxcr3*$^{-/-}$ and *Cxcr3*$^{+/+}$ mice (1:1 mix; 1 × 10$^6$ cells total). Tumors were dissected after mCXCL10 intratumoral injection as described for **e**. Representative plots are shown indicating the strategy for discriminating transferred cells on the basis of congenic markers: pmel-1 infiltrates from *Cxcr3*$^{-/-}$ (Thy-1.1$^+$Thy-1.2$^+$) and *Cxcr3*$^{+/+}$ (Thy-1.1$^+$Thy-1.1$^+$) mice among host CD8$^+$ T cells (Thy-1.2$^+$Thy-1.2$^+$). NS, not significant; *$P < 0.05$. In **b**–**f**, each circle represents a single mouse. Significance was determined by Mann-Whitney statistical test. Data are from one experiment (**a**,**b**) or are pooled from three (**f**) or two (**c**–**e**) independent experiments.

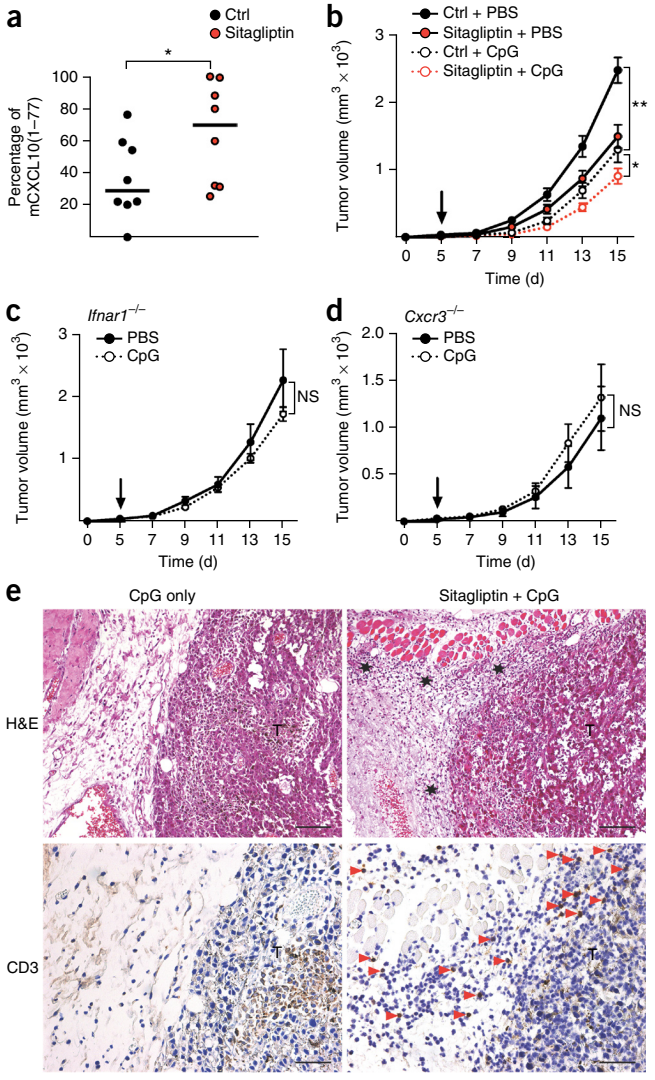


**Figure 6** DPP4 inhibition protects adjuvant-induced CXCL10 and improves tumor immunity. (**a**–**e**) WT (**a**,**b**,**e**), *Ifnar1*$^{-/-}$ (**c**) and *Cxcr3*$^{-/-}$ (**d**) mice fed with control or sitagliptin chow were subcutaneously injected with B16F10 cells. Mice were given an intratumoral injection of 5 μg CpG-A or PBS at the time points indicated by arrows in **b**–**d**. Six hours after CpG-A injection, tumors were dissected and mCXCL10 expression was determined in tumor homogenates. The graph in **a** represents the percentage of mCXCL10(1–77) among total mCXCL10. Each circle represents one mouse. Tumor volumes are shown in line graphs (data represent mean ± s.e.m.; $n = 11$ (**b**) and 5 (**c**,**d**) mice; $^{*}P < 0.01$, $^{**}P < 0.0001$). (**e**) Histological analysis of tumors dissected 18 h after intratumoral CpG injection. H&E, hematoxylin and eosin. The lower panels show CD3 immunolabeling. T, tumor. Stars denote areas of high inflammation. Red arrowheads indicate infiltrating CD3$^{+}$ cells. Images are representative of $n = 11$ mice per group. Scale bars, 100 μm. Significance was determined by Mann-Whitney test (**a**) or two-way ANOVA (**b**–**d**). Data are pooled from two independent experiments (**a**,**b**) or are representative of two experiments (**c**–**e**).

the intact form of mCXCL10 (i.e., mCXCL10(1–77)) and for the presence of isoleucine and proline as its N-terminal residues. The quantity of mCXCL10(1–77) measured when DPP4 was inhibited (**Fig. 4d** and **Supplementary Fig. 5a**) was markedly higher than that in control animals. Similar results were observed in CpG-A–treated *Dpp4*$^{-/-}$ mice (**Supplementary Fig. 5b**). As an additional control, we demonstrated that sitagliptin treatment in *Dpp4*$^{-/-}$ mice did not have an additive effect, again excluding off-target activity of the drug (**Supplementary Fig. 5c**). Intravenous CpG-A injection also induced the expression of mCCL2, mCCL22 and mCCL3. Although the concentrations of mCCL3 were not considerably different between the treatment groups, the quantity of plasma mCCL2 was higher in sitagliptin-treated mice than in control mice (**Supplementary Fig. 5d**), a result that correlates with high sensitivity of mCCL2 to DPP4 truncation (**Supplementary Fig. 2c**). DPP4 inhibition also modulated the plasma concentration of mCCL22, yet in that instance there was a marked decrease in mCCL22 expression (**Supplementary Fig. 5d**). Indeed, DPP4-mediated N-terminal truncation of mCCL22 renders the chemokine inaccessible for scavenging by the atypical chemokine receptor D6 (ref. 23), which helped us interpret this result. These data support DPP4-mediated cleavage as an *in vivo* mechanism for regulating multiple chemokines, with direct evidence of preservation of the bioactive form of CXCL10 (among other chemokines).

To directly test the role of DPP4 in CXCL10-mediated immune-cell trafficking, we injected recombinant mCXCL10 into the peritoneal cavities of wild-type mice fed with control or sitagliptin chow in order to study the chemokine-mediated migration of leukocytes. The peritoneal cavities of these mice showed high DPP4 activity that was significantly inhibited by sitagliptin treatment (**Fig. 5a**,**b**). Notably, mCXCL10 injection did not induce significant infiltration of CXCR3-expressing T cells in control mice, which suggested rapid catabolism of the administered chemokine (**Fig. 5c** and **Supplementary Fig. 6a**). By contrast, inhibition of DPP4 enhanced mCXCL10-mediated T cell infiltration (**Fig. 5c** and **Supplementary Fig. 6a**). Additionally, we observed that plasma membrane expression of CXCR3 on migrating T cells was lower in sitagliptin-treated mice than in control mice (**Fig. 5d** and **Supplementary Fig. 6b**). We interpreted this as a result of DPP4 inhibition enhancing *in vivo* CXCL10-mediated CXCR3 internalization. This effect was observed locally at the site of mCXCL10 injection but not systemically, as indicated by the unaltered CXCR3 expression on peripheral blood T cells (**Supplementary Fig. 6c**). These findings were replicated in *Dpp4*$^{-/-}$ mice, which showed higher lymphocyte migration after intraperitoneal injection of mCXCL10 than did wild-type animals (**Supplementary Fig. 6d**). As CXCL10 has also been proposed to act as an antagonist of CCR3-mediated leukocyte migration[24], we analyzed the recruitment of CCR3-expressing eosinophils. Control and sitagliptin-fed mice injected with mCXCL10 did not show differential recruitment of polymorphonuclear cells into the peritoneal cavity (**Supplementary Fig. 6e**).

In parallel with studies using recombinant mCXCL10, we evaluated the effects of intraperitoneal injection of mCXCL9 (insensitive to DPP4-mediated truncation) and mCCL5 (sensitive to $NH_2$-terminal truncation). With mCXCL9, we observed migration of NK cells into the peritoneal cavity, but consistent with a lack of the DPP4 consensus motif, no increase in lymphocyte migration was observed in *Dpp4*$^{-/-}$ animals (**Supplementary Fig. 7a**). Similar to observations in experiments with mCXCL10, intraperitoneal injection of mCCL5 induced enhanced lymphocyte migration in *Dpp4*$^{-/-}$ animals (**Supplementary Fig. 7b**). We also evaluated the effect of DPP4 inhibition on intraperitoneal thioglycollate-induced inflammation and leukocyte migration. In this model, DPP4 inhibition did not alter the magnitude of leukocyte migration. Thioglycollate stimulated the migration of neutrophils, monocytes and eosinophils, but no differences were observed between sitagliptin-treated mice and control mice (**Supplementary Fig. 8a**,**b**). Thioglycollate did not induce lymphocyte trafficking (**Supplementary Fig. 8c**), probably

accounting for the lack of a DPP4 phenotype. Together these data establish DPP4 as an *in vivo* regulator of chemokine-mediated lymphocyte trafficking.

To extend these results to the migration of lymphocytes into the tumor microenvironment, we tested whether mCXCL10 injection was also able to enhance leukocyte trafficking into the tumor parenchyma. Specifically, we injected mCXCL10 into day 7 melanoma tumors growing in mice fed with either control or sitagliptin chow. Day 7 tumors were selected because DPP4 inhibition has not yet established differential trafficking at that time point (as seen when comparing PBS-treated control mice with PBS-treated sitagliptin-fed mice; **Fig. 5e**). When mCXCL10 was injected into control mice, we did not observe any increase in lymphocyte migration (**Fig. 5e**). This was consistent with the high degree of intratumoral expression of DPP4 (**Fig. 1a**). Sitagliptin treatment resulted in enhanced CXCL10 recruitment of T cells and NK cells into the tumor parenchyma (**Fig. 5e**), whereas trafficking of B cells, regulatory T cells, eosinophils and neutrophils was unchanged (**Supplementary Fig. 9**).

To test for a role for CXCR3 expression, we carried out adoptive cell transfer of gp100 tumor antigen–specific $CD8^+$ T cells (referred to as pmel-1 T cells). Congenic markers were used to track transferred cells. CXCR3-sufficient (Thy-$1.1^+$ pmel-1) and -deficient (Thy-$1.1^+$Thy-$1.2^+$$CXCR3^-$ pmel-1) T cells were mixed at a ratio of 1:1 and transferred into wild-type Thy-$1.2^+$ B16F10 tumor–bearing animals. T cell trafficking was evaluated 12–14 h after mCXCL10 injection into the tumor. CXCL10-mediated trafficking of pmel-1 cells into the B16F10 tumors was enhanced by DPP4 inhibition and showed complete dependence on CXCR3 expression (**Fig. 5f**). Together these data establish that DPP4 inhibition results in the protection of bioactive CXCL10 and enhanced migration of CXCR3-expressing T cells into sites of inflammation and into the parenchyma of growing tumors.

### DPP4 inhibition improves the response to immunotherapy

On the basis of the defined mechanism of action of sitagliptin monotherapy, we predicted that enhanced lymphocyte trafficking could be combined with other immunotherapeutic strategies, especially those that generate high quantities of CXCL10 or that depend on CXCR3-expressing effector T cells. As a first test of our hypothesis, we evaluated the combination of adjuvant therapy and sitagliptin treatment. We selected CpG ODN because it has been used in human trials and is known to induce high expression of endogenous CXCL10 (ref. 25,26). As discussed above, bioactive plasma mCXCL10 produced upon CpG treatment was protected by DPP4 inhibition (**Fig. 4c**,**d**). Similarly, CpG induced high expression of intratumoral CXCL10 (median concentration, ~300 ng per gram of tumor homogenate), and sitagliptin administration protected the full-length form of the molecule (**Fig. 6a**). CpG-A injection also increased the intratumoral expression of mCCL2 and mCCL22, but no notable differences were seen between control and sitagliptin-treated animals (data not shown). Supporting the role of CpG-A as a potent antitumor immune modulator, a single intratumoral injection was sufficient to induce a delay in B16F10 tumor growth, with an additive effect seen when mice were treated with sitagliptin (**Fig. 6b**). CpG-mediated tumor immunity was dependent on signaling of type I interferon receptors and on CXCR3 expression (**Fig. 6c**,**d**). Immunohistochemistry was used to evaluate lymphocyte migration after treatment with CpG, given alone or in combination with sitagliptin. We observed modest $CD3^+$ lymphocyte infiltration of the tumors in CpG only–treated mice, and the tumor capsule remained intact (**Fig. 6e**). By contrast, the addition of sitagliptin resulted in a striking increase in tumor inflammation and T cell recruitment (**Fig. 6e**). We also observed that the tumor capsule was disrupted in mice receiving the DPP4 inhibitor, probably as a result of the enhanced inflammation. These data suggest that inhibition of DPP4 can be used to stabilize biologically active CXCL10, enhancing T cell migration into the tumor parenchyma as a strategy for enhancing adjuvant-based tumor immunity.

We next evaluated DPP4 inhibition in combination with adoptive T cell therapy. Because B16F10 melanoma is refractory to pmel-1 cell adoptive transfer[27], we used an ovalbumin (OVA)-expressing line called MO4 (B16F10 transfected with OVA) that can be recognized by $CD8^+$ OT1 T lymphocytes[28]. Sitagliptin and adoptive cell transfer monotherapies (sitagliptin + PBS and control chow + OT1, respectively) both resulted in a significant delay in B16F10-OVA tumor growth (**Fig. 7a**). When these therapies were used in combination, we observed a synergistic effect, with >80% reduction in tumor size at day 15, as compared with the ~50% inhibition seen with either monotherapy regimen alone (**Fig. 7a**).

Finally, we studied the combination of sitagliptin and checkpoint blockade (anti-PD1 and anti–CTLA-4) in the CT26 tumor model. Sitagliptin monotherapy resulted in delayed CT26 tumor growth (**Fig. 7b**). Although treatment with a combination of sitagliptin and anti-PD1 did not lead to improved tumor immunity as compared with that observed with anti-PD1 monotherapy, we did observe a significant delay in tumor growth after treatment with sitagliptin plus anti–CTLA-4 as compared with growth after treatment with anti–CTLA-4 alone (**Fig. 7b**). The most striking effects were those of triple therapy—sitagliptin given

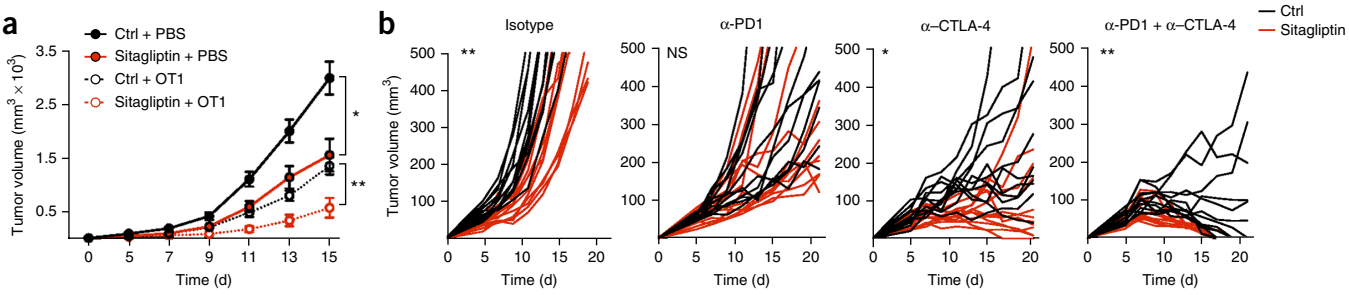


**Figure 7** Combination therapy established DPP4 inhibition as a general mechanism for improving tumor immunity. (**a**) C57BL/6 mice were fed with control or sitagliptin chow before subcutaneous injection of B16F10-OVA cells. On day 3 after tumor-cell injection, mice received an adoptive transfer of OT1 $CD8^+$ T cells or PBS. Data represent mean ± s.e.m.; $n = 6$ mice per group; $^*P < 0.05$, $^{**}P < 0.01$. (**b**) BALB/c mice were fed with control or sitagliptin chow before subcutaneous injection of CT26 cells. On days 3, 6 and 9 after tumor implantation, mice were given intraperitoneal injections of the respective control isotype antibodies (200 μg rat anti-IgG2a + 100 μg rat anti-IgG2b), 200 μg anti-PD1, 100 μg anti–CTLA-4 or a combination of 200 μg anti-PD1 and 100 μg anti–CTLA-4. Each line represents one mouse ($n = 11$–12 mice per group; $^*P < 0.01$, $^{**}P < 0.005$). Significance was determined by two-way ANOVA. Data are representative of two experiments (**a**) or are pooled from two independent experiments (**b**).

in combination with antibodies to both CTLA-4 and PD1—which resulted in 100% of the mice rejecting their tumor by day 21, whereas double therapy with anti–CTLA-4 plus anti-PD1 cured only 42% of the mice during the same period of time (**Fig. 7b**). In summary, our data provide conclusive *in vivo* evidence that DPP4 regulates chemokine trafficking and that its inhibition can be used to enhance the response to current tumor immunotherapy regimens.

## DISCUSSION

To our knowledge, our study provides the first direct evidence for a role of DPP4 as an *in vivo* regulator of CXCL10-mediated lymphocyte trafficking, with relevance for tumor immunity and immunotherapy. By treating mice with an orally active inhibitor of DPP4 enzymatic activity, we demonstrated preservation of full-length CXCL10 that resulted in enhanced T cell migration to inflammatory sites. After DPP4 inhibition, we also augmented the efficacy of naturally occurring and immunotherapy-based tumor immunity. This work places the upregulation and/or induction of DPP4 expression by some tumors in a new context and establishes chemokine post-translational modification as a key immunomodulatory step that can be targeted therapeutically to enhance inflammation.

DPP4 belongs to a family of six pleotropic serine proteases that cleave the N-terminal two amino acids of proteins and peptides[5]. Their roles in regulating biological processes are dictated by their expression patterns and the targeted substrate. Fibroblast activation protein–α (FAP, also known as seprase) and DPP4 are the two cell-surface-expressed enzymes with catalytic domains facing the extracellular space[29]. In the case of DPP4, but not of FAP, high amounts of soluble protein can be found in the plasma and urine of healthy individuals[6,30]. In addition to DPP4's well-studied ability to regulate incretin hormones, *in vitro* biochemical studies have shown that DPP4 can cleave up to 36 chemokines and cytokines possessing a putative truncation site for DPP4 (i.e., the presence of proline in the penultimate position of the N terminus)[31], with stromal-derived factor 1 (also known as CXCL12) being the most substantive *in vivo* example[21,32]. Although a possible role for DPP4 in the regulation of immune cell migration has been suggested, *in vivo* data have not been established, and the concept of post-translational modification as a means of regulating leukocyte trafficking has been largely overlooked by the community, although a few studies were able to identify truncated forms of chemokines in biological samples[32,33]. Indeed, to define DPP4 as an *in vivo* regulator of chemokine-mediated leukocyte trafficking, it was essential to provide definitive evidence of $NH_2$-terminal truncation of *in vivo* substrates.

We chose to study lymphocyte trafficking to tumors because there have been several examples of upregulated or induced DPP4 expression in the context of malignant transformation[7,34]. In some instances the tumor cell itself expresses DPP4, and in other examples the tumor cells do not expresses the enzyme and instead induce its expression in the surrounding tumor stroma[35]. Prior experimental studies have evaluated dipeptidylpeptidases as targets for tumor therapy; however, these studies have been limited by their use of chemical inhibitors that block the activity of both DPP4 and FAP[36,37]. As a notable exception, one report showed that DPP4 is upregulated in a model of MEK1-induced skin tumors and that treatment with sitagliptin delays malignant transformation[38]. Although that study suggests that DPP4 inhibition might be synergistic with interleukin 1 (IL-1) receptor antagonist therapy, the authors do not consider a role for the regulation of lymphocyte trafficking. Instead, they hypothesize that blood glucose levels might alter tumor-cell proliferation. In light of our findings, we can rule out a role for immune-independent mechanisms, as DPP4 inhibition in *Rag2*$^{-/-}$, *Cxcr3*$^{-/-}$ and *Cxcl10*$^{-/-}$ mice did not have a beneficial effect. Because FAP has been reported to be an oncogene[37] and work suggests that FAP-expressing carcinoma-associated fibroblasts contribute to tumor growth[39], we were careful to exclude this as an alternative regulator of tumor immunity in our models.

Post-translational modification of intracellular proteins is fundamental for cellular biology processes such as signal transduction and chromatin organization; however, the role of protein modification in the extracellular space is poorly understood. Several families of enzymes have been reported to modify the structure and/or function of chemokines[40]. Although DPP4-mediated truncation of several chemokines abrogates their chemoattractive functions[3,4], N-terminal truncation of CXCL5 and COOH-terminal truncation of CXCL7 have been shown to enhance their *in vitro* chemoattractive potential[41,42]. Regarding CXCL10 regulation, a report showed that C-terminal truncation by gelatinase B and neutrophil collagenase (MMP-8) does not affect *in vitro* chemotactic activity[43]. Moreover, peptidylarginine deaminases can citrullinate CXCL10, which modestly reduces the migration of T cells, and they may alter the interaction of CXCL10 with heparin sulfate–binding proteins[44]. Our study of dipeptidylpeptidase N-terminal truncation provided experimental evidence that post-translational modification of CXCL10 has *in vivo* biological significance. Future studies will be required to elucidate the role of additional post-translational modifications, which may affect chemokine activity in the context of inflammation and immune activation.

Regarding the application of our findings to tumor immunotherapy, we note that the field has witnessed a rebirth in the past few years, with recent approval of CTLA-4 and PD-1 inhibitors for the treatment of melanoma, as well as several successful high-profile clinical trials[45]. Moreover, immune adjuvants (e.g., CpG) have been directly injected into tumors as a means to enhance the function of antigen-presenting cells and support T cell priming[26]. Limiting the efficacy of these strategies, tumors have evolved mechanisms to resist the action of incoming lymphocytes and promote immunosuppression[46]. Our results suggest that DPP4 could participate in restricting lymphocyte access to the tumor parenchyma by modifying the proinflammatory chemokine CXCL10. On the basis of this, we imagine considerable opportunities for combination therapy involving the addition of DPP4 inhibitors to existing tumor immunotherapy protocols. This innovative approach to enhancing lymphocyte trafficking into tumors may be readily combined with current practices, including T cell adoptive therapy (in instances where the transferred T cells mediate killing)[47–49], intratumoral injection of Toll-like receptor ligands[25,26] or checkpoint blockade[50,51]. In fact, there is a remarkable opportunity for the application of this approach, as DPP4 inhibitors are widely used in the clinic. More than 30 million people are currently taking DPP4 inhibitors to protect the agonist forms of the incretin hormones, highlighting their safety profile and the potential for rapid translation to other therapeutic purposes[9]. In sum, we posit post-translational modification of chemokines as a general mechanism of immune regulation and propose that therapeutic control of these processes could provide robust strategies by which to enhance or inhibit immune responses.

## METHODS

Methods and any associated references are available in the online version of the paper.

*Note: Any Supplementary Information and Source Data files are available in the online version of the paper.*

ACKNOWLEDGMENTS

We thank S. Amigorena, P. Bousso, S. Turley and D. DiGregorio for critical reading of the manuscript. We also thank G. Hangoc (Department of Microbiology and Immunology, Indiana University School of Medicine, Indianapolis, Indiana, USA) for providing the *Dpp4*$^{-/-}$ mice and C. Reis e Sousa (Immunobiology Laboratory, The Francis Crick Institute, London, UK) for the B16F10-OVA tumor cells. We thank M.A. Nicola (Plateforme d'imagerie dynamique, Institut Pasteur, Paris, France) for providing FVB CAG-luciferase transgenic mice. We acknowledge C. Hollande, D. Duffy, A. Casrouge, V. Bondet, V. Mallet, M. Buckwalter, T. Canton, M.A. Nicola and F. Cretien for advice and support. Funding was provided by the Institut Pasteur (Pasteur-Roux post-doctoral fellowship to R.B.d.S.), the Pasteur Foundation (fellowship to M.E.L.), the Ligue Contre le Cancer (M.L.A.), the Fondation ARC pour la recherche sur le cancer (M.L.A.) and the French government's Invest in the Future Program, managed by the Agence Nationale de la Recherche (LabEx Immuno-Onco (R.B.d.S., M.E.L., N.Y., M.A.I. and M.L.A.)).

AUTHOR CONTRIBUTIONS

R.B.d.S. and M.L.A. designed the study. R.B.d.S. and M.E.L. designed, carried out and analyzed experiments. L.F. conducted histological experiments. N.Y. and M.A.I. provided technical and intellectual assistance. R.B.d.S. and M.L.A. wrote the manuscript. M.L.A. supervised the study.

COMPETING FINANCIAL INTERESTS

The authors declare no competing financial interests.



1. Rot, A. & von Andrian, U.H. Chemokines in innate and adaptive host defense: basic chemokinese grammar for immune cells. *Annu. Rev. Immunol.* **22**, 891–928 (2004).
2. Weber, M. *et al.* Interstitial dendritic cell guidance by haptotactic chemokine gradients. *Science* **339**, 328–332 (2013).
3. Mortier, A., Van Damme, J. & Proost, P. Overview of the mechanisms regulating chemokine activity and availability. *Immunol. Lett.* **145**, 2–9 (2012).
4. Proost, P. *et al.* Amino-terminal truncation of CXCR3 agonists impairs receptor signaling and lymphocyte chemotaxis, while preserving antiangiogenic properties. *Blood* **98**, 3554–3561 (2001).
5. Bongers, J., Lambros, T., Ahmad, M. & Heimer, E.P. Kinetics of dipeptidyl peptidase IV proteolysis of growth hormone-releasing factor and analogs. *Biochim. Biophys. Acta* **1122**, 147–153 (1992).
6. Durinx, C. *et al.* Molecular characterization of dipeptidyl peptidase activity in serum: soluble CD26/dipeptidyl peptidase IV is responsible for the release of X-Pro dipeptides. *Eur. J. Biochem.* **267**, 5608–5613 (2000).
7. Stecca, B.A. *et al.* Aberrant dipeptidyl peptidase IV (DPP IV/CD26) expression in human hepatocellular carcinoma. *J. Hepatol.* **27**, 337–345 (1997).
8. Kajiyama, H. *et al.* Increased expression of dipeptidyl peptidase IV in human mesothelial cells by malignant ascites from ovarian carcinoma patients. *Oncology* **63**, 158–165 (2002).
9. Karagiannis, T., Boura, P. & Tsapas, A. Safety of dipeptidyl peptidase 4 inhibitors: a perspective review. *Ther. Adv. Drug Saf.* **5**, 138–146 (2014).
10. Lambeir, A.M. *et al.* Kinetic investigation of chemokine truncation by CD26/dipeptidyl peptidase IV reveals a striking selectivity within the chemokine family. *J. Biol. Chem.* **276**, 29839–29845 (2001).
11. Casrouge, A. *et al.* Evidence for an antagonist form of the chemokine CXCL10 in patients chronically infected with HCV. *J. Clin. Invest.* **121**, 308–317 (2011).
12. Riva, A. *et al.* Truncated CXCL10 is associated with failure to achieve spontaneous clearance of acute hepatitis C infection. *Hepatology* **60**, 487–496 (2014).
13. Ragab, D. *et al.* CXCL10 antagonism and plasma sDPPIV correlate with increasing liver disease in chronic HCV genotype 4 infected patients. *Cytokine* **63**, 105–112 (2013).
14. Christopherson, K.W. II, Cooper, S. & Broxmeyer, H.E. Cell surface peptidase CD26/DPPIV mediates G-CSF mobilization of mouse progenitor cells. *Blood* **101**, 4680–4686 (2003).
15. Oravecz, T. *et al.* Regulation of the receptor specificity and function of the chemokine RANTES (regulated on activation, normal T cell expressed and secreted) by dipeptidyl peptidase IV (CD26)-mediated cleavage. *J. Exp. Med.* **186**, 1865–1872 (1997).
16. Fridman, W.H. *et al.* Prognostic and predictive impact of intra- and peritumoral immune infiltrates. *Cancer Res.* **71**, 5601–5605 (2011).
17. Pagès, F. *et al.* Immune infiltration in human tumors: a prognostic factor that should not be ignored. *Oncogene* **29**, 1093–1102 (2010).
18. Mortier, A., Gouwy, M., Van Damme, J. & Proost, P. Effect of posttranslational processing on the *in vitro* and *in vivo* activity of chemokines. *Exp. Cell Res.* **317**, 642–654 (2011).
19. Groom, J.R. & Luster, A.D. CXCR3 ligands: redundant, collaborative and antagonistic functions. *Immunol. Cell Biol.* **89**, 207–215 (2011).
20. Strieter, R.M., Kunkel, S.L., Arenberg, D.A., Burdick, M.D. & Polverini, P.J. Interferon gamma-inducible protein 10 (IP-10), a member of the C-X-C chemokine family, is an inhibitor of angiogenesis. *Biochem. Biophys. Res. Commun.* **210**, 51–57 (1995).
21. Christopherson, K.W. II, Hangoc, G., Mantel, C.R. & Broxmeyer, H.E. Modulation of hematopoietic stem cell homing and engraftment by CD26. *Science* **305**, 1000–1003 (2004).
22. Forssmann, U. *et al.* Inhibition of CD26/dipeptidyl peptidase IV enhances CCL11/eotaxin-mediated recruitment of eosinophils *in vivo*. *J. Immunol.* **181**, 1120–1127 (2008).
23. Bonecchi, R. *et al.* Differential recognition and scavenging of native and truncated macrophage-derived chemokine (macrophage-derived chemokine/CC chemokine ligand 22) by the D6 decoy receptor. *J. Immunol.* **172**, 4972–4976 (2004).
24. Loetscher, P. *et al.* The ligands of CXC chemokine receptor 3, I-TAC, Mig, and IP10, are natural antagonists for CCR3. *J. Biol. Chem.* **276**, 2986–2991 (2001).
25. Pashenkov, M. *et al.* Phase II trial of a toll-like receptor 9-activating oligonucleotide in patients with metastatic melanoma. *J. Clin. Oncol.* **24**, 5716–5724 (2006).
26. Krieg, A.M. CpG still rocks! Update on an accidental drug. *Nucleic Acid Ther.* **22**, 77–89 (2012).
27. Overwijk, W.W. *et al.* Tumor regression and autoimmunity after reversal of a functionally tolerant state of self-reactive CD8$^+$ T cells. *J. Exp. Med.* **198**, 569–580 (2003).
28. Budhu, S. *et al.* CD8$^+$ T cell concentration determines their efficiency in killing cognate antigen-expressing syngeneic mammalian cells *in vitro* and in mouse tissues. *J. Exp. Med.* **207**, 223–235 (2010).
29. Gorrell, M.D. *et al.* Structure and function in dipeptidyl peptidase IV and related proteins. *Adv. Exp. Med. Biol.* **575**, 45–54 (2006).
30. Wilson, M.J. *et al.* Elevation of dipeptidylpeptidase IV activities in the prostate peripheral zone and prostatic secretions of men with prostate cancer: possible prostate cancer disease marker. *J. Urol.* **174**, 1124–1128 (2005).
31. Ou, X., O'Leary, H.A. & Broxmeyer, H.E. Implications of DPP4 modification of proteins that regulate stem/progenitor and more mature cell types. *Blood* **122**, 161–169 (2013).
32. Antonsson, B., De Lys, P., Dechavanne, V., Chevalet, L. & Boschert, U. *In vivo* processing of CXCL12α/SDF-1α after intravenous and subcutaneous administration to mice. *Proteomics* **10**, 4342–4351 (2010).
33. Favre-Kontula, L. *et al.* Quantitative detection of therapeutic proteins and their metabolites in serum using antibody-coupled ProteinChip arrays and SELDI-TOF-MS. *J. Immunol. Methods* **317**, 152–162 (2006).
34. Carbone, A. *et al.* The expression of CD26 and CD40 ligand is mutually exclusive in human T-cell non-Hodgkin's lymphomas/leukemias. *Blood* **86**, 4617–4626 (1995).
35. Kacar, A. *et al.* Stromal expression of CD34, α-smooth muscle actin and CD26/DPPIV in squamous cell carcinoma of the skin: a comparative immunohistochemical study. *Pathol. Oncol. Res.* **18**, 25–31 (2012).
36. Adams, S. *et al.* PT-100, a small molecule dipeptidyl peptidase inhibitor, has potent antitumor effects and augments antibody-mediated cytotoxicity via a novel immune mechanism. *Cancer Res.* **64**, 5471–5480 (2004).
37. Santos, A.M., Jung, J., Aziz, N., Kissil, J.L. & Pure, E. Targeting fibroblast activation protein inhibits tumor stromagenesis and growth in mice. *J. Clin. Invest.* **119**, 3613–3625 (2009).
38. Arwert, E.N. *et al.* Upregulation of CD26 expression in epithelial cells and stromal cells during wound-induced skin tumour formation. *Oncogene* **31**, 992–1000 (2012).
39. Lee, J., Fassnacht, M., Nair, S., Boczkowski, D. & Gilboa, E. Tumor immunotherapy targeting fibroblast activation protein, a product expressed in tumor-associated fibroblasts. *Cancer Res.* **65**, 11156–11163 (2005).
40. Moelants, E.A., Mortier, A., Van Damme, J. & Proost, P. *In vivo* regulation of chemokine activity by post-translational modification. *Immunol. Cell Biol.* **91**, 402–407 (2013).
41. Mortier, A. *et al.* Posttranslational modification of the NH2-terminal region of CXCL5 by proteases or peptidylarginine deiminases (PAD) differently affects its biological activity. *J. Biol. Chem.* **285**, 29750–29759 (2010).
42. Ehlert, J.E., Gerdes, J., Flad, H.D. & Brandt, E. Novel C-terminally truncated isoforms of the CXC chemokine β-thromboglobulin and their impact on neutrophil functions. *J. Immunol.* **161**, 4975–4982 (1998).
43. Van den Steen, P.E., Husson, S.J., Proost, P., Van Damme, J. & Opdenakker, G. Carboxyterminal cleavage of the chemokines MIG and IP-10 by gelatinase B and neutrophil collagenase. *Biochem. Biophys. Res. Commun.* **310**, 889–896 (2003).
44. Loos, T. *et al.* Citrullination of CXCL10 and CXCL11 by peptidylarginine deiminase: a naturally occurring posttranslational modification of chemokines and new dimension of immunoregulation. *Blood* **112**, 2648–2656 (2008).
45. Hodi, F.S. *et al.* Improved survival with ipilimumab in patients with metastatic melanoma. *N. Engl. J. Med.* **363**, 711–723 (2010).
46. Kerkar, S.P. & Restifo, N.P. Cellular constituents of immune escape within the tumor microenvironment. *Cancer Res.* **72**, 3125–3130 (2012).
47. Schmitt, T.M., Ragnarsson, G.B. & Greenberg, P.D. T cell receptor gene therapy for cancer. *Hum. Gene Ther.* **20**, 1240–1248 (2009).
48. June, C.H. Adoptive T cell therapy for cancer in the clinic. *J. Clin. Invest.* **117**, 1466–1476 (2007).
49. Gattinoni, L., Powell, D.J. Jr., Rosenberg, S.A. & Restifo, N.P. Adoptive immunotherapy for cancer: building on success. *Nat. Rev. Immunol.* **6**, 383–393 (2006).
50. Leach, D.R., Krummel, M.F. & Allison, J.P. Enhancement of antitumor immunity by CTLA-4 blockade. *Science* **271**, 1734–1736 (1996).
51. Iwai, Y. *et al.* Involvement of PD-L1 on tumor cells in the escape from host immune system and tumor immunotherapy by PD-L1 blockade. *Proc. Natl. Acad. Sci. USA* **99**, 12293–12297 (2002).

## ONLINE METHODS

**Mice.** Wild-type C57BL/6, CD45.2, Thy1.2 and BALB/c mice were obtained from Charles River, France. Wild-type C57BL/6, CD45.1, *Rag2*$^{-/-}$, *Cxcr3*$^{-/-}$, *Ifnar1*$^{-/-}$, *Dpp4*$^{+/-}$, *Dpp4*$^{-/-}$, *Cxcl10*$^{-/-}$, *Ccr5*$^{-/-}$, pmel-1 Thy-1.1$^{+}$Thy-1.1$^{+}$, OT1 and FVB-Tg(CAG-luciferase) mice were bred in the mouse facility at Institut Pasteur. Male pmel-1 Thy-1.1$^{+}$Thy-1.1$^{+}$ mice were crossed with female *Cxcr3*$^{-/-}$ Thy-1.2$^{+}$Thy-1.2$^{+}$ mice to obtain first-generation males that were pmel-1 *Cxcr3*$^{-/-}$ Thy-1.1$^{+}$Thy-1.2$^{+}$. Mice used were 7–12 weeks old. For inhibition of DPP4 activity *in vivo*, mice were fed with chow (SAFE) formulated to contain 1.1% sitagliptin (Merck). Sitagliptin food was administered to mice before treatments, unless otherwise stated in figure legends. Mice were maintained in a specific-pathogen-free facility, and all experimental protocols were approved by the Comité d'Éthique pour l'Expérimentation Animale (Ethics Committee for Animal Experimentation), Paris.

**Mass spectrometry.** Recombinant mDPP4, mCXCL10, mCXCL9, mCXCL11, mCCL2, mCCL3, mCCL4, mCCL5, mCXCL12 and mCCL22 were purchased from Peprotech. For surface-enhanced laser desorption/ionization time-of-flight (SELDI-TOF) mass spectrometry, chemokines were incubated in the presence or absence of 10 nM mDPP4 for 30 min at 37 °C. The digested product was applied to an H4 protein chip according to the manufacturer's instructions and analyzed with the ProteinChip Systems Series 4000 (Ciphergen). Data were analyzed with CiphergenExpress software.

**Model of trafficking into the peritoneal cavity.** Wild-type and *Dpp4*$^{-/-}$ mice were intraperitoneally injected with PBS or 1 µg of mCXCL10, mCXCL9 or mCCL5 (all from Peprotech). Mice were killed and peritoneal cells were collected in 10 ml of PBS 12–14 h after injection unless stated otherwise. For thioglycollate-induced peritonitis, mice were intraperitoneally injected with thioglycollate 3% wt/vol 24 h before the collection of peritoneal cells.

**DPP4 enzymatic activity.** For evaluation of DPP4 enzymatic activity, mice were bled and plasma samples were collected after centrifugation of the blood. For measurements of DPP4 activity in tumor homogenates, tumors growing in mice were dissected, weighed and homogenized in PBS supplemented with protease inhibitor cocktail (Roche). Soluble extracts were collected after centrifugation of tumor homogenates. We assessed DPP4 activity in the peritoneal cavity by collecting peritoneal washes in 1.5 ml of PBS. DPP4 activity was measured with the DPPIV-Glo Protease Assay (Promega). For evaluation of DPP4 activity *in vivo*, FVB-Tg(CAG-luc) mice were fed with control or sitagliptin chow 24 h before intraperitoneal injection of 10 mM Gly-Pro-aminoluciferin (Promega). Bioluminescence images were acquired with a XENOGEN (IVIS system, PerkinElmer) 5 min after injection.

**Tumor growth *in vivo*.** B16F10 and M04 tumor cells (ovalbumin-expressing B16F10 cells, a gift from C. Reis e Sousa, Francis Crick Institute) were cultured in DMEM (Gibco) supplemented with 10% FCS (PAA), 0.1 mM non-essential amino acids, 1 mM sodium pyruvate, 10 mM HEPES, 70 µM β-mercaptoethanol and 23 µg/ml gentamycin (all from Gibco). CT26 colon carcinoma cells were cultured in RPMI medium (Gibco) supplemented as described for DMEM. Cells for injections were passaged one to two times after being thawed before use. Wild-type and genetically modified mice were subcutaneously injected with $2 \times 10^5$ B16F10 cells or $5 \times 10^5$ CT26 cells in the shaved right flank. Mice received an intratumoral injection of 1 µg recombinant mCXCL10, 5 µg CpG-A in the cationic lipid DOTAP or vehicle control. For blocking of chemokines and chemokine receptors, wild-type mice were intraperitoneally injected with 100 µg of hamster anti-mCXCR3 (clone CXCR3-173, BioLegend), 100 µg of hamster anti-mCCR5 (clone HM-CCR5, BioLegend), 50 µg of rat anti-mCXCL10 (clone 134013, R&D Systems) and 20 µg of rat anti-mCXCR4 (clone 2B11/CXCR4, BD Biosciences) or with the respective isotype antibodies (hamster IgG antibody (clone HTK888, BioLegend, used as a control for mCXCR3 and mCCR5 blockage), rat IgG2a antibody (clone 54447, R&D Systems, used as a control for mCXCL10 blockade) and rat IgG2b antibody (clone A95-1, BD Biosciences, used as a control for mCXCR4 blockade)). Intraperitoneal injection was done 1 d before and 4, 8 and 12 d after tumor-cell injection. For CXCL10 neutralization, antibodies were injected on days 2, 5, 8 and 11 after tumor-cell injection. For immunotherapy protocols, mice were intraperitoneally injected with 100 µg of mouse anti–CTLA-4 (clone 9D9, Bio X Cell), 200 µg of anti-PD1 (clone RMP1-14, Bio X Cell), a combination of 100 µg anti–CTLA-4 and 200 µg anti-PD1, or control isotypes (100 µg rat anti-IgG2b (clone MPC-11) and 200 µg rat anti-IgG2a (clone 2A3), both from Bio X Cell) on days 3, 6 and 9 after tumor cell implantation. For adoptive cell transfer experiments, splenocytes from pmel-1 Thy-1.1$^{+}$Thy-1.1$^{+}$, *Cxcr3*$^{-/-}$ Thy-1.1$^{+}$Thy-1.2$^{+}$ pmel-1 or OT1 mice were activated *ex vivo* by incubation with 1 nM human gp100 (for pmel-1 cells) or SIINFEKLL (for OT1 cells) peptides for 1 h at room temperature with agitation. Splenocytes were then washed and resuspended in R10 medium supplemented with 30 U/mL recombinant human IL-2. CD8$^{+}$ T cells were expanded for 6–7 d before being used. For analysis of tumor infiltrates, activated transgenic pmel-1 CD8$^{+}$ T cells from *Cxcr3*$^{+/+}$ Thy-1.1$^{+}$Thy-1.1$^{+}$ and *Cxcr3*$^{-/-}$ Thy-1.1$^{+}$Thy-1.2$^{+}$ mice were mixed in a 1:1 ratio (total: $1 \times 10^6$ cells) and injected intravenously into gender-matched tumor-bearing mice (3 d after tumor-cell injection). For analysis of tumor growth, activated OT1 cells were injected intravenously ($1 \times 10^5$ cells per mouse) into gender-matched tumor-bearing mice 3 d after tumor-cell injection. Tumor height and width were measured with a caliper, and tumor volume was calculated (elliptical volume = width$^2$ × height × 0.523). The model of metastatic melanoma was achieved by intravenous injection of $2 \times 10^5$ B16 F10 tumor cells. Fifteen days after tumor-cell injection, lungs were dissected and placed in Fekete's solution, and metastatic foci were counted. Lungs with more than 100 metastatic nodules were counted as having 100 nodules.

**Flow cytometry.** Fluorochrome-conjugated antibodies used were anti-mouse CD3 (clone 145-2C11, BD Biosciences), anti-mouse CD8 (clone 53-6.7, BD Biosciences), anti-mouse CD4 (clone RM4-5, BD Biosciences), anti-mouse NK1.1 (clone PK136, BD Biosciences), anti-mouse CD49b (clone DX5, BD Biosciences), anti-mouse CD25 (clone PC61, BD Biosciences), anti-mouse CD45R (B220, clone RA3-6B2, eBiosciences), anti-mouse Ly-6G (clone 1A8, BD Biosciences), anti-mouse Ly-6C (clone AL-21, BD Biosciences), anti-mouse CD11b (clone M1/70, BD Biosciences), rat anti-mouse Siglec-F (clone E50-2440, BD Biosciences), anti-mouse MHC class II I-A/I-E (clone M5/114.15.2, eBiosciences), anti-mouse CD45.2 (clones 56-0454-82 (eBiosciences) and 109830 (BioLegend)), anti-mouse Thy-1.1 (clone HIS51, eBiosciences), anti-mouse Thy-1.2 (clone 53-2.1, eBiosciences), anti-mouse DPP4 (CD26, clone H194-112, eBiosciences), anti-mouse CXCR3 (clone CXCR3-173, BD Biosciences) and anti-F4/80 (clone CI:A3-1, AbDserotec). For exclusion of dead cells, Live/Dead fixable Aqua reagent (Invitrogen) was used. Cell suspensions were incubated with mouse CD16/CD32 Fc–blocking antibodies (BD Biosciences) before incubation with fluorochrome-conjugated antibodies. For analysis of peritoneal cavity infiltrates, cells were washed and incubated with a cocktail of fluorochrome-conjugated antibodies. For analysis of tumor infiltrates, B16F10 and CT26 tumors were collected and digested in PBS supplemented with 2.7 mg/ml Collagenase (Roche) and 23 U/ml DNase I (Invitrogen) for 30 min at 37 °C. Digestion was terminated by PBS supplemented with 2% FCS and 5 mM EDTA (Gibco). Tumor-cell suspensions were obtained after filtration over a 70-µm cell strainer. For the determination of cell numbers, AccuCheck Counting Beads reagent (Invitrogen) was used. Flow cytometry was done with a BD LSRFortessa or a BD Canto cytometer, with DIVA software. Computer analysis was done with FlowJo (Treestar).

**Histology.** B16F10 tumors were dissected and fixed in JB fixative (zinc acetate, 0.5%; zinc chloride, 0.05%; and calcium acetate, 0.05% in Tris buffer, pH 7) for 48 h before being embedded in low-melting-point paraffin (polyethylene glycol distearate, Sigma). 5-µm-thick paraffin sections were deparaffinized in absolute ethanol, air dried, and stained with hematoxylin-eosin or used for immunolabeling. For immunohistochemistry, the following primary antibodies were used: anti-CD3 (rabbit anti-human, clone A0452, DAKO, Carpinteria, CA) and anti-CD31 (rat anti-mouse, clone 1/75e, BD Pharmingen, Franklin Lake, NJ, USA). CD31-immunolabeled sections were digitalized with a Zeiss Axio Scan Z.1 at ×20 magnification. For histomorphometry of blood vessels, CD31-positive profiles were manually delineated on digitalized images with the "area" tool of the Zen software (Zeiss) at a magnification of 30%. The whole tumor surface was also delineated in the same way at a magnification of 2%. The mean number of blood vessels per square millimeter and mean vessel area were then calculated for each group of mice.





doi:10.1038/ni.3201

***In vitro* T cell migration and CXCR3 internalization assays.** For evaluation of T cell migration with different mCXCL10 isoforms, $5 \times 10^5$ activated pmel-1 $CD8^+$ T cells were resuspended in 100 µl of HBSS medium (Gibco) supplemented with 0.1% BSA and placed in the upper chamber of a 96-well Transwell plate containing 5-µm pores (Corning). T cells were allowed to migrate into the lower chamber, where no chemokine (medium only) or full-length mCXCL10(1–77) and DPP4-truncated mCXCL10(3–77) were added. For evaluation of CXCR3 expression, activated pmel-1 cells were incubated with chemokines in a 96-well U-bottom plate. After 1.5 h, the number of cells migrating to the lower chamber and expression of surface CXCR3 were evaluated by flow cytometry.

**ELISA/Luminex assays.** For detection of mCXCL10(1–77), Maxisorp plates (Nunc) were coated with 4 µg/ml capturing antibody to mCXCL10 (MAB466, R&D Systems) in PBS and incubated overnight at 4 °C. Plates were washed twice with 300 µl of PBS. Blocking was done with 1% BSA (protease free, Gibco) in PBS for 2 h at room temperature. Plates were washed three times with 300 µl of 0.05% Tween-20 in PBS. Tumor and plasma samples were diluted in 1% BSA and incubated for 2 h at room temperature. To obtain a standard curve, and to control for the cross-reactivity of the detection antibody, we incubated dilutions of recombinant mCXCL10 (Peprotech) and DPP4-digested mCXCL10(3–77) in parallel. For the detection of mCXCL10(1–77), biotinylated anti-mCXCL10(1–77) (AbDSerotec, 0.5 µg/ml, clone AbD17185.1), Streptavidin-HRP (BD Biosciences) and 1-Step Ultra TMB (Thermo Scientific) were used. Enzymatic reactions were stopped with HCL 1N, and plates were read at 450 nm in a Lab-systems Multiskan MS (Thermo) reader. For the detection of total mCXCL10, the mCXCL10 DuoSet ELISA kit (R&D Systems) or a combination of capturing anti-mCXCL10 (MAB466, R&D Systems) and biotinylated anti-mCXCL10 (BAF466, R&D Systems) was used, unless otherwise indicated. Detection of mDPP4, mCCL22 and mCXCL12 was done with Duoset ELISA kits (R&D Systems). Detection of mVEGF, mCCL2 and mCCL3 was done with a multiplex kit (Invitrogen).

**Statistical analysis.** In all instances, statistical tests were done with Prism GraphPad.